

# Transition of phase continuity induced by crosslinking and interfacial reaction during reactive processing of compatibilized PVC/SBR blends

Shuihan Zhu and Chi-Ming Chan\*

*Department of Chemical Engineering, Advanced Engineering Materials Facility, The Hong Kong University of Science and Technology, Clear Water Bay, Kowloon, Hong Kong, Republic of China*

*(Received 20 October 1997; accepted 6 February 1998)*

Blends of 50 wt% of poly(vinyl chloride) (PVC) and 40 wt% of styrene butadiene rubber (SBR) with 10 wt% of acrylonitrile butadiene rubber (NBR) as the compatibilizer were prepared in a Haake mixer. An inversion of phase continuity was observed when the sulfur concentration was changed from 0.0 to 2.0 parts per hundred parts of resins (phr) in the blends containing an NBR with an acrylonitrile content of 29.5 wt% (NBR-29). The SBR phase, which is continuous in the unvulcanized blend, changes progressively into the dispersed phase as sulfur concentration increases. This is explained by the viscosity increase of the rubber caused by crosslinking. There is no phase inversion as a result of increasing sulfur concentration when the compatibilizer NBR-29 was replaced by an NBR with an acrylonitrile content of 40 wt% (NBR-40). The SBR phase is discrete in the unvulcanized blend with NBR-40 as the compatibilizer.

A change in phase continuity occurs during processing of the vulcanized PVC/NBR-29/SBR (50/10/40) blends. A torque peak in the torque curve during processing is correlated to the transition of the PVC phase continuity. There is a gradual increase in the torque curve after the torque peak. The rubber particle size decreases as a result of such a post-peak increase in the torque. The torque peak and the post-peak increase in the torque are absent in the case of the binary blends (PVC/NBR and PVC/SBR). The post-peak increase in the torque is attributed to the interfacial reaction between SBR and NBR that resides in the PVC phase.

A novel method developed recently was applied to study the interface development during processing. An interface with a higher rubber concentration develops during processing of the compatibilized blends. © 1998 Elsevier Science Ltd. All rights reserved.

(Keywords: PVC/SBR blends; crosslinking; interfacial reaction)

## INTRODUCTION

Morphological features, such as phase continuity, dispersion size and distribution, dispersion shape, and interface, play crucial roles in the properties of immiscible polymer blends<sup>1–5</sup>. Phase continuity is the most important morphological features. For example, in an emulsion, which can be regarded as a model for immiscible polymer blends<sup>1</sup>, electrical conductivity measurements are used to determine the types of emulsions (water-in-oil type or oil-in-water type), based on an abrupt jump in electrical conductance, which occurs at the phase inversion threshold<sup>2,3</sup>. Similarly, the moduli of immiscible polymer blends show a maximum change in the transition region of phase continuity as the blend composition changes<sup>4,5</sup>.

When polymer blends are prepared by melt-mixing, development and formation of morphology are dependent on both thermodynamic and rheological parameters such as interfacial tension<sup>6</sup>, composition<sup>7,8</sup>, viscosity<sup>8–12</sup> and elasticity<sup>13,14</sup>. The morphological development during processing has attracted much attention owing to the importance of the rheological parameters, such as viscosity ratio and elasticity ratio of the blend components, in deciding the final morphology of the materials<sup>15–17</sup>. A

transition of phase continuity may occur when the viscosities of the blend components change as a result of the gradient in heat conductance during processing. For instance, a specific melting sequence of blend components can lead to an observable phase inversion during mixing when the blend components have significantly different melting or softening temperatures. Shih<sup>18</sup> and Sundararaj<sup>19</sup> studied several blends in which the minor component has a lower softening point than the major one. During blending, the component with a lower transition temperature melted first, and coated the particles of the major component. As the major component melted, the particles were stretched into sheets, and formed a continuous phase, leading to a phase inversion. A torque peak, which was observed during mixing either at an isothermal or temperature ramp condition, corresponds to a phase inversion.

Maximum viscosity related to a phase inversion caused by the change in the blend composition has been observed<sup>20</sup>. In trying to relate the blend viscosity to its composition, Utracki<sup>21</sup> proposed a general viscosity equation (see equations (1)–(3)) for immiscible polymer blends:

$$\log \eta = \Delta \log \eta^E + \log \eta_L \quad (1)$$

The first term on the right-hand side of equation (1) is the

\* To whom correspondence should be addressed

excess contribution defined by:

$$\Delta \log \eta^E = \eta_{\max} \left[ 1 - \frac{(\phi_1 - \phi_{1p})^2}{(\phi_1 \phi_{2p}^2 + \phi_2 \phi_{1p}^2)} \right] \quad (2)$$

where  $\eta_{\max}$  is an empirical parameter determining the magnitude of the positive deviation behaviour (PDB) effect;  $\phi_{1p}$  and  $\phi_{2p}$  (the phase inversion threshold) are volume fractions of phases 1 and 2 at which the respective phase becomes continuous;  $\phi_i$  ( $i = 1$  or  $2$ ) is the volume fraction of component  $i$  in the blend. When  $\phi_i = 0$ ,  $\Delta \log \eta^E = 0$ ; as  $\phi_i$  increases,  $\Delta \log \eta^E$  increases progressively to its maximum  $\eta_{\max}$  at  $\phi_i = \phi_{ip}$ . An increase in the dispersion size and dispersion phase continuity has been noted as the blend composition approaches the phase inversion threshold value<sup>8</sup>. Thus, it is believed that an increase in phase continuity contributes to the increase in the viscosity of the blends.

The second term on the right hand side of equation (1) is the additive contribution of the components and the interfacial slip expressed by the following equation:

$$\log \eta_L = \log [1 - \beta(\phi_1 \phi_2)^{1/2}] - \log \left[ \frac{\phi_1}{\eta_1} + \frac{\phi_2}{\eta_2} \right] \quad (3)$$

where  $\beta = \beta(\sigma_{12})$  is the interlayer slip factor which is dependent on shear stress;  $\eta_1$  and  $\eta_2$  are viscosities of the components 1 and 2, respectively. Weak interfacial adhesion results in slip at the interface. If the interfacial slip is large enough, the maximum viscosity corresponding to a phase inversion may be obscured or disappear<sup>20</sup>. On the other hand, an interfacial reaction will prevent the interfacial slip and augment the maximum viscosity effect<sup>21</sup>. In fact, a higher torque peak corresponding to a phase inversion has been noted for the more reactive components in a study on polymer blends with several reactive components<sup>18,19</sup>.

When the composition of polymer blends is close to the phase inversion threshold (mostly  $\phi_{ip} = 40 \sim 60$  vol%), the processing parameters are very important in deciding the final morphology of the materials<sup>22</sup>. In the present study, 50 wt% of poly(vinyl chloride) (PVC) and 40 wt% styrene-butadiene rubber (SBR) were blended with 10 wt% of acrylonitrile-butadiene rubber (NBR) as a compatibilizer. Since NBR is compatible with PVC, the two phases, of which one phase is SBR and the other is a blend of PVC and NBR, are expected to have a volume fraction close to 0.50. During mixing, the rubbers (both SBR and NBR) are vulcanized, and covulcanization between NBR and SBR may occur at the interface of the SBR and PVC phases. The objective of the present study is to investigate the morphology changes induced by vulcanization. The morphological development of the vulcanized blends was correlated with the torque trace recorded online during mixing, which is a measure of the blend viscosity. The interface evolution during mixing was also studied using a method developed recently for this blend<sup>23</sup>.

## EXPERIMENTS

Fifty parts by weight of poly(vinyl chloride) (PVC,  $K$  value 67) and 50 parts of styrene-butadiene rubber (SBR, Nipol 1502, Zeon Chemicals) were melt-blended in a Haake mixer 600. This blend was designated as the PVC/SBR (50/50) blend. Two acrylonitrile-butadiene rubbers (NBR) used as compatibilizers contained 29.5 (NBR-29, Nipol 1053, Zeon Chemicals) and 40 wt% (NBR-40, Nipol 1041, Zeon

Chemicals) of acrylonitrile. To prepare the compatibilized blends, SBR was replaced by NBR in the amount of 5 and 10 wt%, designated as the PVC/NBR/SBR (50/5/45) and (50/10/40) blends, respectively. The binary PVC/NBR-29 (50/50) blend was prepared for the purpose of comparison with the ternary blends in the torque curve. The PVC/NBR (50/10) blends were also prepared for the measurement of the viscosities of the blend components. Zinc and barium stearates were used as stabilizers for PVC. The curing package contained sulfur as the primary crosslinking agent, mercaptobenzothiazole (MBT) as the accelerator, and ZnO as the activator. The total weight of the materials was controlled, allowing the melt volume to be kept at *ca.* 70% of the mixer volume for maximum convective mixing. The Banbury rotors were operated at 30 rpm. The torque required to operate the rotors during mixing was recorded every 6 s. The temperature of the mixer chamber wall was controlled at 150°C by compressed air cooling and electric heating. The actual temperature was measured by a thermocouple, which was mounted in contact with the melt inside the mixer chamber. The blending lasted for 22 min, and the compound was hot-pressed into plaques for further analysis.

The rheological properties were measured using a parallel-plate viscometer (Rheometrics RMS 800) in a dynamic mode. The temperature was controlled at 155°C. The frequency sweep was performed at a strain of 0.5% from 1 to 100 rad/s.

A transmission electron microscope (JEM 100 CXII, JEOL) was applied to study the morphology of the sample. Samples for transmission electron microscopy (TEM) were obtained by cryomicrotomy the materials at  $-120^\circ\text{C}$  with a diamond knife. The nominal advance for cutting was set at 80 nm after initial trimming. The ultrathin sections were collected on a copper grid, and stained by a solution of 2 wt% OsO<sub>4</sub>. A thin carbon coating was deposited on the grid to prevent electrostatic charging. Observation of the interface development was performed on unstained thin sections of the samples. The contrast change was recorded by taking micrographs at several electron irradiation times under a TEM electron beam. The greyscale of the TEM micrographs were measured using an image analysis software (Quantimet 600, Leica). The measurement system was calibrated with a standard length scale bar. In each measurement, a line was selected across the interface, and the greyscale in each pixel was recorded. The normalized greyscale was obtained by divide the measured greyscale by the largest greyscale value in the line.

## RESULTS AND DISCUSSION

### Phase inversion

Figure 1a–d show TEM micrographs of the PVC/NBR-29/SBR (50/10/40) blends with four sulfur concentrations. All these blends show a two-phase microstructure. NBR has been shown to be miscible with PVC<sup>24</sup>, hence it is expected that NBR is fully dispersed in the PVC phase. Even though both SBR and NBR have double bonds, which can react with OsO<sub>4</sub>, the dark areas are SBR because the density of the double bonds is much higher in the SBR phase than in the PVC phase. Figure 1a shows the morphology of the unvulcanized blends, indicating that SBR is the continuous phase while PVC is the discrete phase. This suggests that the viscosity of SBR is lower than the other component—a blend of PVC and NBR-29 which will be discussed in a later

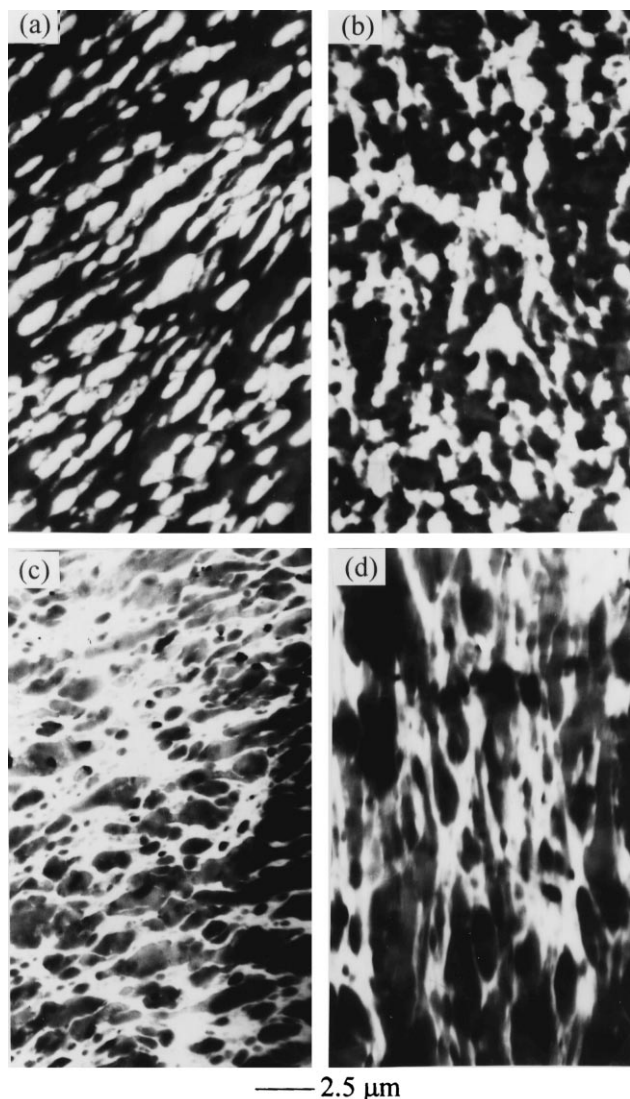


**Figure 1** TEM micrographs of the PVC/NBR-29/SBR (50/10/40) blends: (a) unvulcanized; (b) vulcanized by S/MBT/ZnO = 0.5/0.5/1.0 phr; (c) vulcanized by S/MBT/ZnO = 1.0/1.0/2.0 phr; and (d) vulcanized by S/MBT/ZnO = 2.0/0.5/4.0 phr

section. At 0.5 phr of sulfur, the blend forms a co-continuous structure (see *Figure 1b*). A phase inversion—the rubber changes from being the continuous phase to being the discrete phase—occurs at sulfur concentration of 1.0 phr, as shown in *Figure 1c*. As the amount of sulfur increases further to 2 phr, the particle size of the crosslinked rubber becomes larger, as shown in *Figure 1d*. This is owing to a higher crosslinking density of the rubber in the blend with a higher sulfur concentration. The highly crosslinked rubber particles are much more difficult to be broken and dispersed.

The morphology of the blends containing NBR-40 as the compatibilizer is shown in *Figure 2a–d*. However, there is no phase inversion as sulfur concentration increases. In the unvulcanized blend, the PVC becomes the continuous phase, as shown in *Figure 2a*. This suggests that one of the components—the PVC/NBR-40 (50/10) blend—has a lower viscosity than SBR, thus than the PVC/NBR-29 (50/10) blend.

#### Viscosities of the blend components in unvulcanized blends

The viscosity ratio of blend components is an important

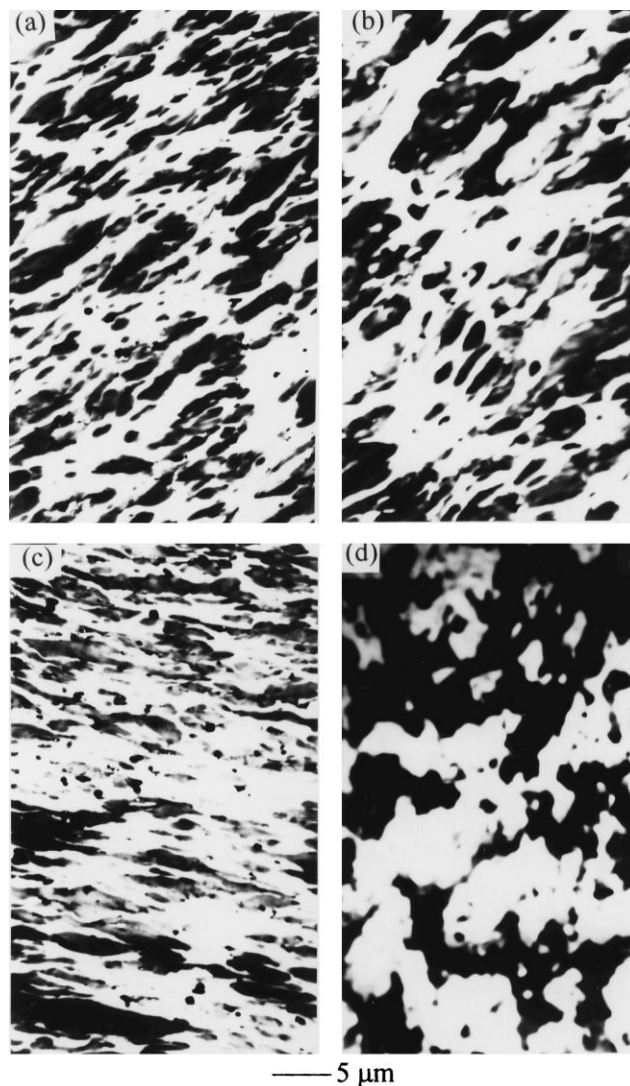


**Figure 2** TEM micrographs of the PVC/NBR-40/SBR (50/10/40) blends: (a) unvulcanized; (b) vulcanized by S/MBT/ZnO = 0.5/0.5/1.0 phr; (c) vulcanized by S/MBT/ZnO = 1.0/1.0/2.0 phr; and (d) vulcanized by S/MBT/ZnO = 2.0/0.5/4.0 phr

factor to determine phase continuity. An empirical equation<sup>7,8</sup> (see equation (4)) that relates the viscosity ratio ( $\lambda = \eta_1/\eta_2$ ) to the phase inversion concentration ( $\phi_{2p}$ ) is given by

$$\phi_{2p} = \frac{1}{1 + \lambda} \quad (4)$$

The volume fraction at phase inversion can be calculated from the viscosity ratio. The component with a lower viscosity tends to form the continuous phase in the blend.

In a Haake mixer, the two counter-rotating rotors are driven by a common shaft with a rotational speed  $N$ , but geared to rotate at a speed ratio of 3 to 2. The local shear rate is not uniform and a nominal average shear rate is obtained by assuming the flow field to be that between two coaxial cylinders<sup>25–28</sup>. Depending upon the material properties tested, the nominal equivalent shear rate at the above conditions is between 0.76 and  $3.7N^{2/6}$ , where  $N$  is the rotational speed of the common shaft in rpm. By applying this relation with  $N = 30$  rpm, the nominal shear rate is calculated to be in the range of 22.8 to  $111 \text{ s}^{-1}$ . Thus, the range of shear rate was chosen from 1 to 100 rad/s to measure the viscosity ratio of the blend components.

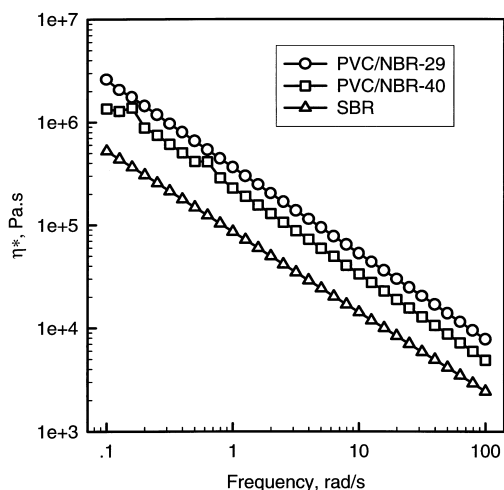


**Figure 3** Dynamic viscosity of the blend components as a function of frequency

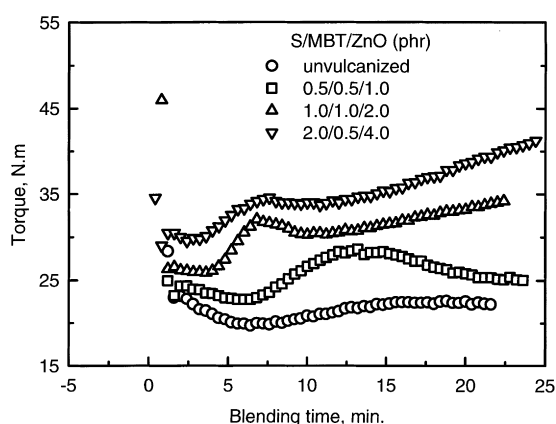


**Figure 4** The torque variation at different mixing times during processing of the PVC/NBR-29/SBR (50/10/40) blends vulcanized by S/MBT/ZnO = 1.0/1.0/2.0 phr. For clarity, the curves were shifted up 5 and 10 N.m, respectively, from the third curve on

PVC is compatible with NBR with AN content ranging from 23 to 45 wt%<sup>24</sup>. Dynamic mechanical analysis and differential scanning calorimetry results show that the glass transition temperature ( $T_g$ ) of PVC in the blends decreases to low temperatures as the NBR content increases, while the  $T_g$  of SBR remains unchanged. These results suggest that most of the NBR resides in the PVC phase. Therefore, the PVC/NBR/SBR (50/10/40) blends can be treated as consisting of two components—SBR and a PVC/NBR (50/10) blend. Figure 3 shows the viscosity change as a function of frequency for the three blend components involved. The PVC/NBR-29 (50/10) blend has the highest viscosity, and SBR has the lowest viscosity among the three materials. From the morphological analysis of the unvulcanized PVC/NBR/SBR (50/10/40) blends, as shown in Figures 1a and 2a, the viscosities for the three components

should be in the order of: PVC/NBR-29 > SBR > PVC/NBR-40. The thermal crosslinking of SBR in the blend during processing, which is confirmed by the torque curve (will be shown in a later section) obtained during processing, may increase the viscosity of the SBR above that of the PVC/NBR-40 blend, but lower than that of the PVC/NBR-29 blend.

Table 1 shows the viscosity ratio of the components of the PVC/NBR-29/SBR (50/10/40) and PVC/NBR-40/SBR (50/10/40) blends calculated using the measured viscosity ratio. Values for  $\phi_{2p}$  (the SBR concentration at phase inversion) were calculated with equation (4) using the viscosity ratios. The volume fraction of SBR  $\phi_2$  in the blends is estimated to be about 0.49 using the density of SBR, PVC and the PVC/NBR (50/10) blend of 0.92, 1.35, and 1.30 g/cm<sup>3</sup>, respectively. Comparing  $\phi_{2p}$  and  $\phi_2$  values leads to the conclusion that SBR should be the continuous phase in all these blends. However, this conclusion is not consistent with our experimental findings because the actual viscosity of the SBR may be higher than those measured values owing to the thermal crosslinking of the SBR. If the viscosity of the SBR is assumed to be twice of those shown in Figure 3, the calculated values for  $\lambda$  and  $\phi_{2p}$  will change accordingly. As shown in Table 1, the SBR in the PVC/NBR-29/SBR (50/10/40) blend will still be the continuous phase until the viscosity of the SBR is further increased by crosslinking. This is exactly what we observed – a phase inversion occurs when the sulfur concentration is above 1.0 phr. However, the SBR in the PVC/NBR-40/SBR (50/10/40) blend is the discrete phase when  $\phi_{2p} > 0.49$ . Hence, further increases in the sulfur concentration will not cause a phase inversion.

Since the degree of crosslinking of the SBR in the blends is unknown, it is impossible to measure the viscosity of the components in the vulcanized blends. Instead, the torque variation during mixing may yield the detail information on the viscosity change of the blend components.

#### Effect of reaction on torque curve during processing

Vulcanization of NBR and SBR is expected to change the torque during processing. Figure 4 shows the torque variations during mixing for an unvulcanized and three vulcanized PVC/NBR-29/SBR (50/10/40) blends. If there is no reaction, the torque will be expected to level off to an equilibrium value as mixing proceeds. In the case of the unvulcanized blend, the torque decreases to a minimum quickly after the initial loading peak. There is a slow increase owing to lightly thermal crosslinking of the SBR in the blend. The difference in the torque values at the minimum and at the end of mixing is approximately 1.3 N.m. This is the contribution from thermal crosslinking of the SBR alone, since the thermal crosslinking of the NBR in the blend cannot be observed on the torque curve (shown in a later section). The assumption made in the previous section that thermal crosslinking increases the viscosity of the SBR in the blend is, thus, confirmed. A quantitative evaluation of the increase in SBR viscosity is difficult on the basis of the torque data owing to large fluctuations in the

**Table 1** The viscosity ratios of the components and the calculated values of  $\phi_{2p}$  of the PVC/NBR-29/SBR (50/10/40) and PVC/NBR-40/SBR (50/10/40) blends

	Component 1 = PVC/NBR-29 (50/10), Component 2 = SBR		Component 1 = PVC/NBR-40 (50/10), Component 2 = SBR	
Experimental data	$\lambda$	$\phi_{2p}$	$\lambda$	$\phi_{2p}$
$\eta_2$ is assumed to be twice of the measured value for SBR	3.3–3.7	0.35–0.23	2.1–2.4	0.33–0.30
	1.6–1.9	0.38–0.35	1.0–1.2	0.50–0.46

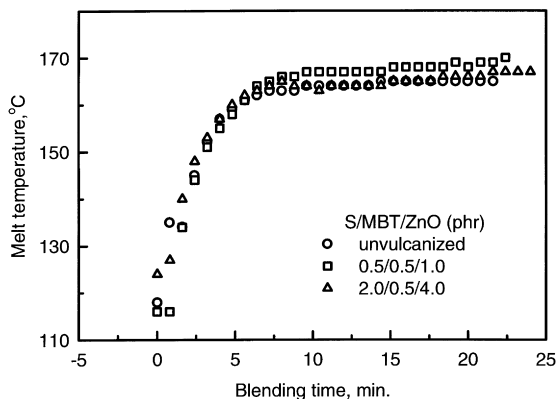


**Figure 5** The temperature variation during processing of both the unvulcanized and vulcanized PVC/NBR-29/SBR (50/10/40) blends

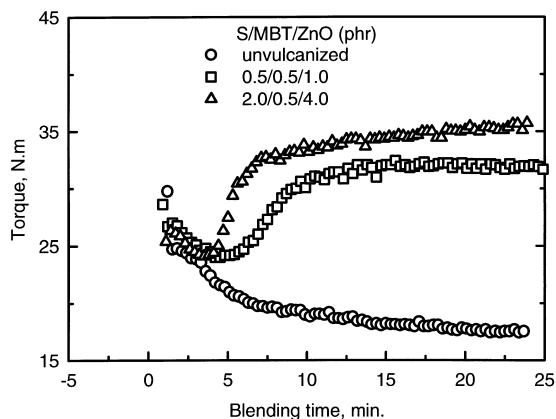


**Figure 6** The torque variation during processing of the PVC/NBR-29 (50/50) blends with different sulfur concentrations

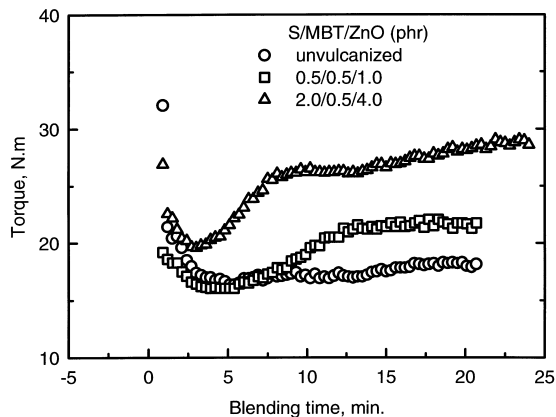


**Figure 7** The torque variation during processing of the PVC/SBR blends (50/50) vulcanized by different concentrations of sulfur

torque values during mixing and the unknown relation between the viscosities of the blend and the components in the complex flow field.

In the case of the PVC/NBR-29/SBR (50/10/40) blend containing 0.5 phr sulfur, a significant increase in the torque is observed. A further increase in sulfur concentration results in an abrupt increase in the torque value, which is followed by a decrease, forming a torque peak. The decrease in the torque lasts for 2–3 min, after that an increase in the torque is observed until the end of mixing.

To interpret the torque curve, the effect of temperature should be considered since the temperature may have a strong influence on the viscosity of the blend components.

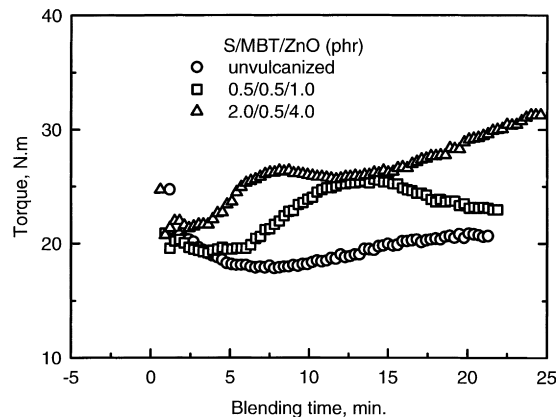


**Figure 8** The torque variation during processing of the PVC/NBR-29/SBR (50/5/45) blends with different sulfur concentrations

Viscous heating and exothermic vulcanization are expected to raise the melt temperature above the set temperature. Variations of the melt temperature during processing of unvulcanized and vulcanized PVC/NBR-29/SBR (50/10/40) blends are shown in *Figure 5*. The temperature increases rapidly in the first few minutes and then levels off 5 min later to an equilibrium value owing to efficient convective heat transport in the mixer. The level-off times for the unvulcanized and vulcanized blends are almost the same. The equilibrium temperatures are a few degrees higher than the set temperature (150°C) owing to viscous heating for the unvulcanized blend. The vulcanized blends have slightly higher melt temperatures than the unvulcanized blend owing to the exothermic reaction and the more intensive dissipative heating of the vulcanized rubber. Once the temperature levels off, it remains constant up to the end of mixing, where the torque is still changing. Thus, the effect of temperature on the torque variation is limited. The reaction taking place during processing and the morphological changes may be the reasons which affect the viscosity and the torque during processing.

#### Covulcanization of SBR and NBR

To discriminate the vulcanization and covulcanization effects on the torque variation during processing, PVC/SBR (50/50) and PVC/NBR (50/50) blends were prepared. The torque curves for the PVC/NBR-29 (50/50) blends are shown in *Figure 6*. There is no indication of thermal crosslinking for the NBR in the blend without sulfur, as the torque stays relatively constant after the initial loading peak. When the blend contains the curing agents, the torque increases abruptly as a result of crosslinking of NBR. An increase in sulfur concentration leads to a faster and larger increase in the torque. The level-off rate is a reflection of the vulcanization rate, and the equilibrium torque value is associated with the degree of crosslinking in the rubber. No torque peak is formed and there is no post-peak increase in the torque, in contrast with those of the ternary blends as shown in *Figure 4*.

*Figure 7* shows the torque curves for the PVC/SBR (50/50) blends with different sulfur concentrations. The unvulcanized blend shows a slow increase after the initial loading peak owing to the thermal crosslinking associated with the SBR. Similar to the PVC/NBR-29 (50/50) blend, an increase in sulfur concentration leads to a faster rate to reach a higher equilibrium torque during processing, indicating a higher vulcanization rate and a

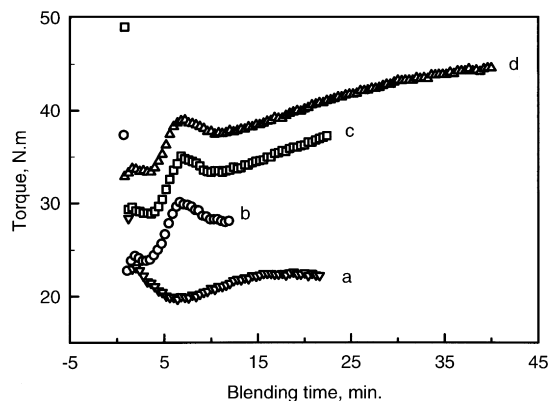


**Figure 9** Torque variation during processing as a function of mixing time for the PVC/NBR-29/SBR (50/10/40) blends (a) unvulcanized blend with a mixing time of 22 min; and vulcanized blend (S/MBT/ZnO = 1.0/1.0/2.0 phr) with a mixing time of: (b) 12 min; (c) 22 min; and (d) 40 min. For clarity, the curves were shifted upwards 4 and 7 N.m, respectively, from the third curve on

higher degree of crosslinking. Similar again to the PVC/NBR-29 (50/50) blend, neither a torque peak nor a post-peak increase in the torque is observed for the blends containing sulfur concentration up to 2 phr.

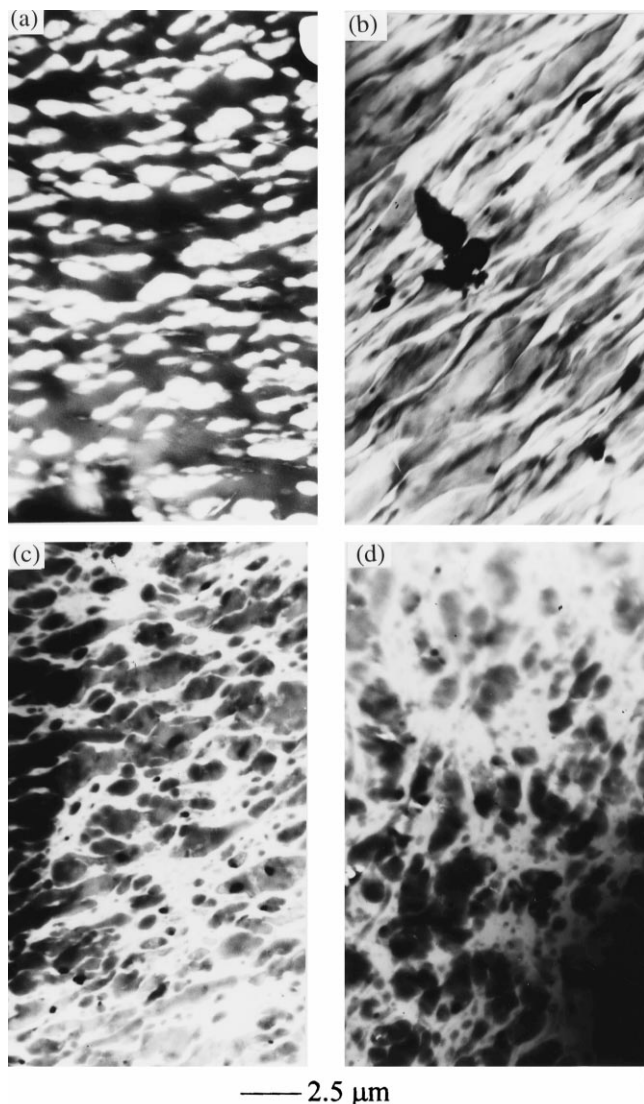


**Figure 10** TEM micrographs of stained samples for the blends a, b, c, and d as shown in Figure 9

To further verify that the torque peak and the post-peak increase in the torque during processing are unique for the ternary PVC/NBR/SBR blends, the NBR-29 concentration was reduced to 5 wt% in the blends. Their torque curves during processing are shown in Figure 8. The curve features are analogous to those of the blends with 10 parts of NBR-29. A torque peak and a post-peak increase in the torque occur when the sulfur increases to 2 phr.

Since the torque peak and the post-peak increase in torque are uniquely associated with the ternary blends, the effect of NBR in the blend should be considered. The NBR which is added to the blend as a compatibilizer to reduce the interfacial tension may cause the morphological changes because it changes the viscosity of PVC owing to its plasticizing effect. As discussed in the Introduction, the morphological changes and the interfacial covulcanization between NBR and SBR will contribute to the viscosity change, thus the torque variation during processing. Therefore, the morphological development and interface evolution during processing were studied.

#### Morphology development during processing

The morphological development as a function of mixing time of the PVC/NBR-29/SBR (50/10/40) blend vulcanized by S/MBT/ZnO = 1.0/1.0/2.0 phr was studied. Three samples were taken at different mixing times, as shown in Figure 9. Blend a is the unvulcanized blend with a mixing time of 22 min, while blends b, c, and d are the vulcanized blends with 12, 22, and 40 min of mixing time, respectively. Blend b was obtained after the torque peak, but before the post-peak increase in the torque; and blend c was obtained in the post-peak increase region in the torque. The TEM micrographs for the blends are shown in Figure 10a–d. The morphology of the unvulcanized blend, which is shown in Figure 10a, indicates that PVC is dispersed in the rubber matrix owing to its higher viscosity than SBR. As a result of vulcanization, the viscosity of SBR increases to the extent close to or higher than that of PVC. Minimization of dissipative energy in flow system will require a reconfiguration of the blend components<sup>29–31</sup>. Figure 10b, which was taken after the torque peak, shows a co-continuous morphology. The PVC phase is deformed and stretched into sheets. As the viscosity of the SBR further increases, the PVC particles are elongated and become the continuous phase (see Figure 10c). With the PVC being the continuous phase which contributes more to the blend viscosity than does the discrete phase, the increase in the blend viscosity as a result of the vulcanization the SBR is expected to slow down or even decrease to form a torque peak. Further increases in mixing time have little effect on the morphology (see Figure 10d).

#### Torque peak and post-peak increase of torque in ternary blends

The torque curves during blending can be understood with the help of the morphological development in vulcanized blends. The torque peak is formed owing to a change in continuity of the PVC phase. This transition of phase continuity is caused by the change in the viscosity ratio during processing as a result of vulcanization.

Based on the fact that the post-peak increase in the torque occurs only in the ternary blends, and that a finer rubber dispersion resulted from a longer mixing time, we arrive at the conclusion that the interfacial covulcanization between NBR and SBR occurs and contributes to the increase in the torque after the torque peak. In fact, the



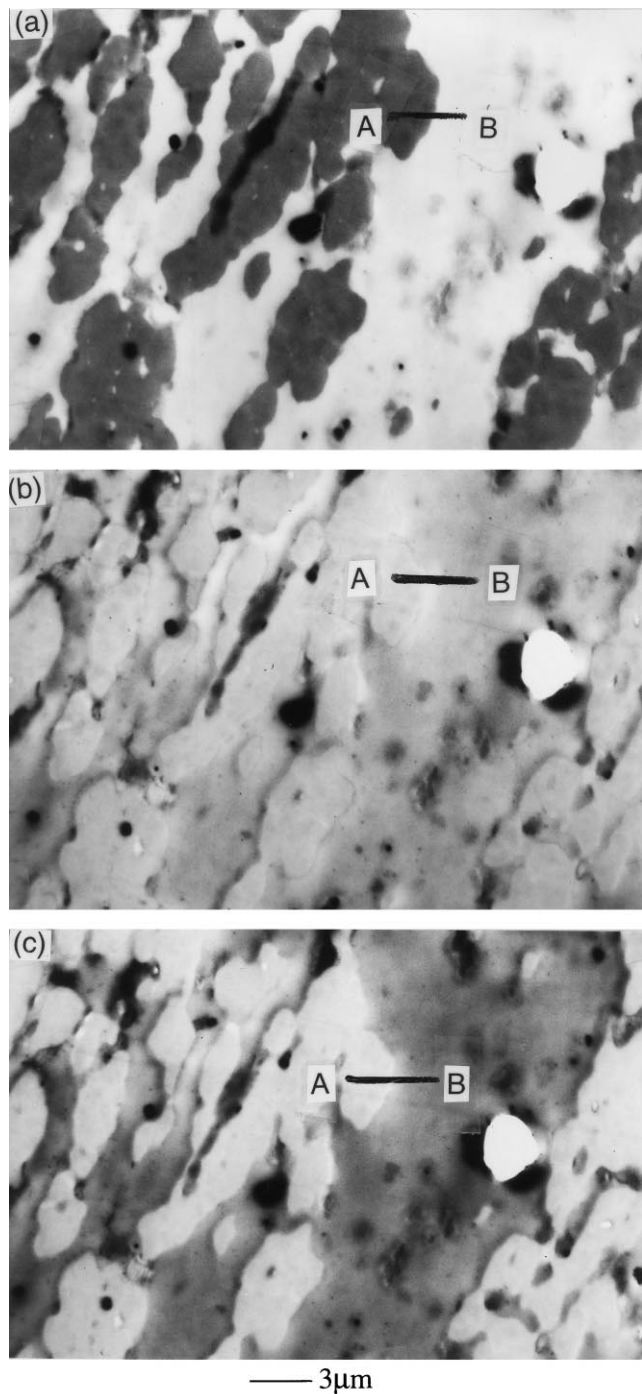


**Figure 11** TEM micrographs of the unstained sample taken at three electron irradiation times: (a) 0.5; (b) 1.0; and (c) 1.5 min. The sample is the PVC/SBR (50/50) blend vulcanized by S/MBT/ZnO = 0.5/0.5/1.0 phr

interfacial reaction can reduce the interlayer slip at the interface. As is obvious from equations (1)–(3), a reduction in the interfacial slip leads to an increase in the viscosity of the blend. As a result of the interfacial reaction, a well-developed interfacial layer is expected to be formed. The interface viscosity, which was introduced by Oldroyd<sup>32,33</sup> in a derivation of emulsion viscosity  $[\eta]$ , is defined by the ratio of surface viscosity to the diameter of the dispersed particles ( $d$ ), as shown in equations (5)–(7).

$$[\eta] = \frac{2.5\lambda' + 1}{\lambda' + 1} \quad (5)$$

$$\text{in which } \lambda' = \frac{\eta_d + \eta_l}{\eta_m} \quad (6)$$

$$\text{where } \eta_l = \frac{2\eta_{ls} + 3\eta_{le}}{5d} \quad (7)$$

The suffixes, d, m, l, s and e in the equations represent dispersion, matrix, interface, shear, and elongation, respectively. The interface viscosity increases effectively the viscosity of the dispersed phase. Verification of the interface development during processing was performed.

#### Interface development

The interface development in the vulcanized PVC/NBR-29/SBR blends involves the migration of the NBR to the interface and the covulcanization between NBR and SBR during processing. The interfacial covulcanization, which increases the torque after the torque peak, requires the contact between NBR and SBR at the interface. The sample obtained before the post-peak increase in the torque has an underdeveloped interface where the contact between NBR and SBR is not fully developed. On the other hand, the sample obtained after a period of interfacial covulcanization is expected to possess a well-developed interface. In order to verify this hypothesis, a novel method developed recently was applied to investigate the interface<sup>23</sup>. This method is based on the observation of unstained blend samples under TEM electron beam irradiation. The contrast of the unstained PVC blends arises from the relatively heavy element Cl. The PVC phase becomes increasingly transparent under the electron beam owing to dehydrochlorination. The contrast deteriorates as a result of the Cl loss. *Figure 11a–c* shows three TEM micrographs of the PVC/SBR (50/50) blend vulcanized by 0.5 phr of sulfur, taken at three different electron irradiation times. The PVC phase is dark initially, while the SBR phase is transparent, as shown in *Figure 11a*. The PVC becomes transparent owing to a decrease in the mass thickness of the PVC areas after the Cl loss. The contrast is inverted in less than 2 min of electron irradiation time.

However, the PVC in the compatibilized PVC/NBR-29/SBR (50/10/40) blend is stabilized owing to the presence of the rubbers in its close proximity<sup>23</sup>. *Figure 12a–c* shows the TEM micrographs of the PVC/NBR-29/SBR (50/10/40) blend vulcanized by S/MBT/ZnO = 1.0/1.0/2.0 phr with 22 min of mixing time (blend c as shown in *Figure 9*). As the electron beam irradiation continues, no contrast inversion is observed. This is because NBR absorbs part of the electron energy, and protects the PVC in close proximity. As a result, dark rings are observed at the interface between the SBR and PVC phases, suggesting that the PVC at the interface is more resistant to electron beam irradiation. The higher resistance of the PVC at the interface to electron beam damage is attributed to a higher rubber concentration in the proximity, which protects the PVC by absorbing the energy of the electron beam.

To provide more quantitative data to support that a contrast inversion indeed has occurred, a line scan to measure the greyscale value (marked by line AB, as shown in *Figure 11*) was made from a dark PVC phase to a light SBR phase. The greyscale value in each pixel was recorded. *Figure 13* shows the normalized greyscale value as the scanner moved from points A to B. Low and high greyscale values present dark and light areas, respectively, in a TEM micrograph. It is obvious from the linescan, as shown in *Figure 13*, a contrast inversion has taken place for the

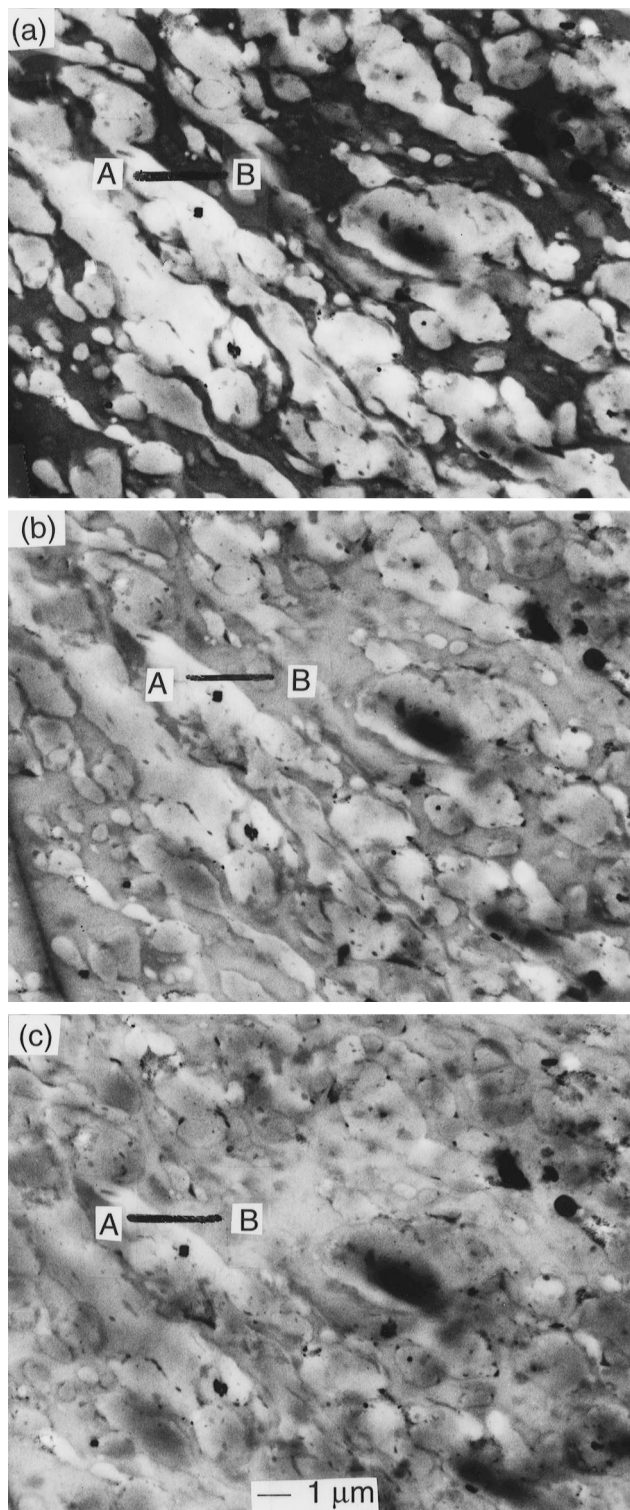


**Figure 12** TEM micrographs of the unstained sample (blend c as shown in Figure 9) taken at three electron irradiation times: (a) 0.5; (b) 1.0; and (c) 1.5 min

uncompatibilized PVC/SBR (50/50) blend as the irradiation time increases. Similar linescans were made on Figure 12 for a compatibilized PVC/SBR-29/SBR (50/10/40) blend. From the results shown in Figure 14, no contrast inversion is observed. In addition, for the TEM micrograph obtained after 1.5 min of irradiation, a peak in the greyscale value is observed. This peak corresponds to a narrow region of dark area in the TEM micrograph (Figure 12c), which is more stable to electron beam irradiation owing to a higher

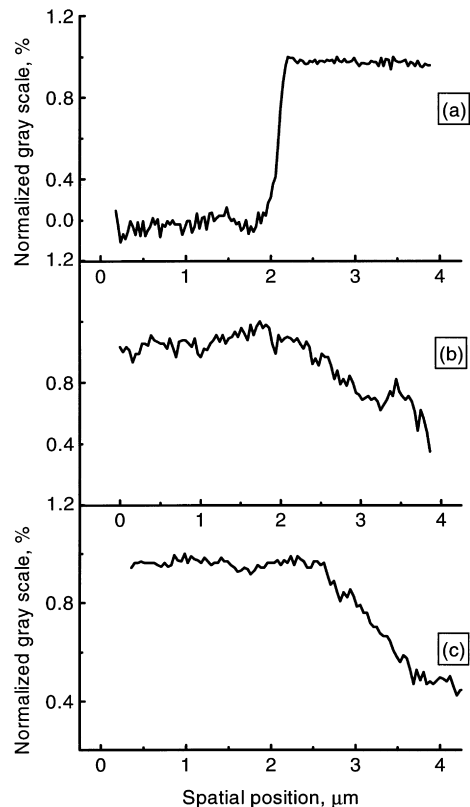


**Figure 13** The normalized greyscale profiles along the three lines in Figure 11a-c

concentration of NBR. The full width at half-maximum height is taken as the thickness of the interface between the PVC and SBR phases. The average value of six measurements made at different locations is  $258 \pm 37$  nm.

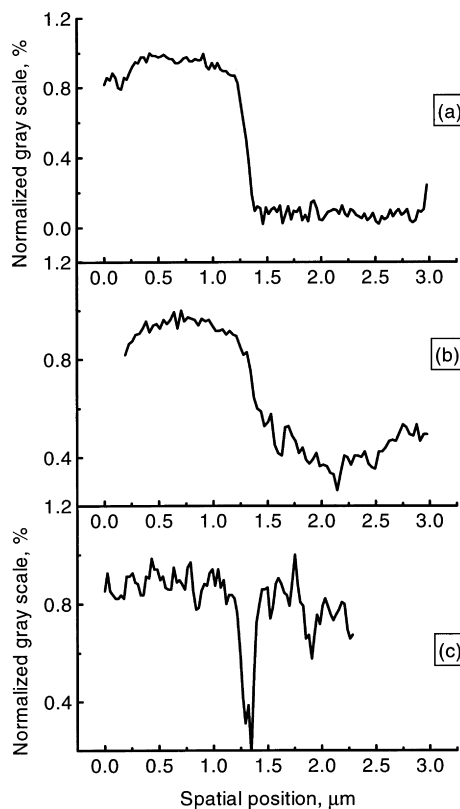


**Figure 14** The normalized greyscale profiles along the three lines in Figure 12a-c



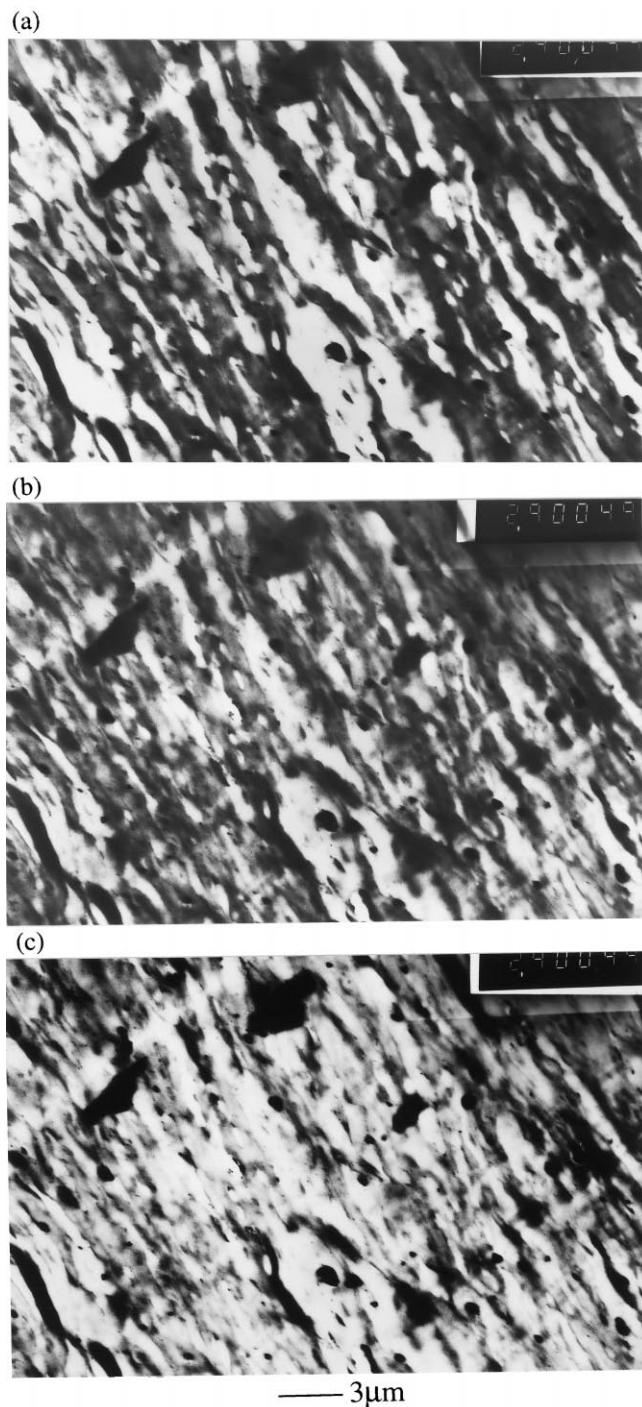


**Figure 15** TEM micrographs of the unstained sample (blend b as shown in *Figure 9*) taken at three electron irradiation times: (a) 0.5; (b) 1.0; and (c) 1.5 min

In the foregoing discussion, we can conclude that NBR is an effective compatibilizer for the PVC/SBR blend. During compounding, the NBR migrates to the interface, facilitating covalent crosslinking with the SBR. The linescans shown in *Figure 14* were made on the blend (blend c as shown in *Figure 9*) which was mixed for 22 min. It would be of interest to find out whether blends with shorter mixing times would have an enhanced NBR concentration at the interface. Blend b (shown in *Figure 9*) which is the same material as blend c except with a shorter mixing time (mixing time = 12 min, before the post-peak increase) was studied by TEM. *Figure 15a–c* shows three TEM micrographs for an unstained sample of blend b at the three

electron irradiation times under the identical conditions used for taking the TEM micrographs shown in *Figure 12*. It is clear from these TEM micrographs that the contrast of the PVC phase deteriorates as electron beam irradiation continues, but not to the extent of having a contrast inversion owing to some stabilizing effect of the NBR in intimate mixing with the PVC. However, no dark rings are observed at the interface between the SBR and PVC phases, indicating that the NBR concentration is not high enough to stabilize the PVC at the interface. These results suggest that the migration of the NBR to the interface takes place after the torque peak and during the post-peak increase. The migration of the NBR is possibly accelerated by covalent crosslinking with the SBR. The increase in tensile strength and elongation-at-break from 15.1 MPa and 63% for blend b to 18.7 MPa and to 100% for blend c, respectively, further supports this argument.

## CONCLUSIONS

- (1) A phase inversion occurs in the PVC/NBR-29/SBR (50/10/40) blends as the sulfur concentration increases, while no phase inversion is observed when NBR-29 is replaced by NBR-40. The change in the phase continuity is explained by the changes in the viscosity ratio of the blend components. During processing of the vulcanized PVC/SBR blends with NBR-29 as the compatibilizer, a transition of the phase continuity occurs when the rubbers are being crosslinked. The morphology evolves from an SBR continuous morphology, to an SBR and PVC co-continuous morphology, and then to a dispersed SBR phase structure.
- (2) The transition of continuity of the PVC phase is correlated to the torque peak observed during processing.
- (3) The interface with a higher rubber concentration develops during blending. The increase in the rubber concentration at the interface between PVC and SBR was detected by TEM studies. The interfacial covalent crosslinking between NBR and SBR accounts for the post-peak increase in torque and helps to reduce the rubber particle size and prevent particle coalescence.

## ACKNOWLEDGEMENTS

This work was supported by the Hong Kong Government Research Council under the grant number of HKUST 583/94E.

## REFERENCES

1. Utracki, L. A., *Polymer Alloys and Blends*. Hanser Publishers, New York, 1989.
2. Salager, J. L., Minana-Perez, M. and Anderez, J. M., *J. Dispersion Sci. Technol.*, 1983, **4**(2), 161.
3. Smith, S. H., Nwosu, S. N., Johnson, G. K. and Lim, K.-H., *Langmuir*, 1992, **8**, 1076.
4. Davies, W. E. A., *J. Phys. D: Appl. Phys.*, 1971, **4**, 318 and 1176.
5. Nielsen, L. E. and Landel, R. F., *Mechanical Properties of Polymers and Composites*. Marcel Dekker, New York, 1994.
6. Wu, S., *Polym. Engng Sci.*, 1987, **27**, 335.
7. Jordhamo, G. M., Manson, J. A. and Sperling, L. H., *Polym. Engng Sci.*, 1986, **26**, 517.
8. Favis, B. D. and Chalifoux, J. P., *Polym. Engng Sci.*, 1987, **27**, 1591.

9. Nelson, C. J., Avgeropoulos, G. N., Weissert, F. C. and Bohm, G. G. A., *Angew. Makromol. Chem.*, 1977, **60/61**, 49.
10. Siegfried, D. L., Thomas, D. A. and Sperling, L. H., *J. Appl. Polym. Sci.*, 1981, **21**, 39.
11. Siegfried, D. L., Thomas, D. A. and Sperling, L. H., *J. Appl. Polym. Sci.*, 1981, **26**, 177.
12. Meijer, H. E. H. and Elemans, P. H. M., *Polym. Engng Sci.*, 1988, **28**, 275.
13. Levett, L., Macosko, C. W. and Pearson, S. D., *Polym. Engng Sci.*, 1996, **36**, 1647.
14. Ghodgaonkar, P. G. and Sundararaj, U., *Polym. Engng Sci.*, 1996, **36**, 1656.
15. Utracki, L. A. and Shi, Z. H., *Polym. Engng Sci.*, 1992, **32**, 1824.
16. Wang, Y., White, J. L. and Szydowski, W., *Int. Polym. Process.*, 1989, **4**, 262.
17. Lim, S. and White, J. W., *Polym. Engng Sci.*, 1994, **34**, 221.
18. Shih, C.-K., *Polym. Engng Sci.*, 1995, **35**, 1688.
19. Sundararaj, U., Macosko, C. W. and Shih, C. K., *Polym. Engng Sci.*, 1996, **36**, 1769.
20. Acierno, D., Curto, D., La Manitia, F. P. and Valenza, A., *Polym. Engng Sci.*, 1986, **26**, 28.
21. Utracki, L. A., *J. Rheol.*, 1991, **35**, 1615.
22. Zhu, S.-H. and Chan, C.-M., SPE Tech. Paper, Ontario, Canada, May 1997.
23. Zhu, S.-H. and Chan, C.-M., *Macromolecules*, 1998, **31**, 1690.
24. Zakrzewski, G. A., *Polymer*, 1973, **14**, 348.
25. Yang, L.-Y., Bigio, D. and Smith, T. G., *J. Appl. Polym. Sci.*, 1995, **58**, 129.
26. Goodrich, J. E. and Porter, R. S., *Polym. Engng Sci.*, 1967, **7**, 45.
27. Blyler, L. L. Jr and Daane, J. H., *Polym. Engng Sci.*, 1967, **7**, 178.
28. Lee, G. C. N. and Purdon, J. R., *Polym. Engng Sci.*, 1969, **9**, 360.
29. Van Oene, H. J., *Colloid Interface Sci.*, 1972, **40**(3), 448-449.
30. Joseph, D. D., Renardy, M. and Renardy, Y., *J. Fluid Mech.*, 1984, **141**, 309.
31. Than, P. T., Rosso, F. and Joseph, D. D., *Int. J. Engng Sci.*, 1987, **25**(2), 189.
32. Oldoyld, J. C., *Proc. R. Soc.*, 1953, **A 218**, 122.
33. Oldoyld, J. C., *Proc. R. Soc.*, 1955, **A232**, 567.